The Astrophysical Journal, 809:54 (7pp), 2015 August 10 doi:10.1088/0004-637X/809/1/54
© 2015. The American Astronomical Society. All rights reserved.

# VERTICAL STRUCTURE OF ADVECTION-DOMINATED ACCRETION FLOWS

Fateme Zahra Zeraatgari[1] and Shahram Abbassi[1,2]
[1] Department of Physics, School of Sciences, Ferdowsi University of Mashhad, Mashhad, 91775-1436, Iran; fzeraatgari@yahoo.com, abbassi@um.ac.ir
[2] School of Astronomy, Institute for Research in Fundamental Sciences (IPM), Tehran, 19395-5531, Iran
*Received 2015 May 27; accepted 2015 July 4; published 2015 August 10*

## ABSTRACT

We solve the set of hydrodynamic equations for optically thin advection-dominated accretion flows by assuming a radially self-similar spherical coordinate system ($r$, $\theta$, $\phi$). The disk is considered to be in steady state and axisymmetric. We define the boundary conditions at the pole and the equator of the disk and, to avoid singularity at the rotation axis, the disk is taken to be symmetric with respect to this axis. Moreover, only the $\tau_{r\phi}$ component of the viscous stress tensor is assumed, and we have set $v_\theta = 0$. The main purpose of this study is to investigate the variation of dynamical quantities of the flow in the vertical direction by finding an analytical solution. As a consequence, we found that the advection parameter, $f^{\rm adv}$, varies along the $\theta$ direction and reaches its maximum near the rotation axis. Our results also show that, in terms of the no-outflow solution, thermal equilibrium still exists and consequently advection cooling can balance viscous heating.

*Key words:* accretion, accretion disks – hydrodynamics

## 1. INTRODUCTION

Accretion onto a compact object such as a black hole is a fundamental phenomenon in the universe and most likely is the primary power source in systems like X-ray binaries, active galactic nuclei, and gamma-ray bursts. Observation of X-ray and gamma-ray emission lines from black hole accretion disks demonstrates the idea of forming a hot atmosphere above the accretion disk or perhaps radiatively inefficient flows (RIAFs; e.g., Blair et al. 1984; Raymond 1993; Jimenez-Garate et al. 2005).

In the standard accretion disk model (Shakura & Sunyaev 1973) the energy released via viscosity is radiated locally and the accreting flow becomes cool very efficiently. Therefore, this model cannot produce a high-energy spectrum and the idea of the existence of a hot corona above the disk is needed to predict such high-energy emissions. In terms of RIAFs, in fact, the heat generated through viscosity is stored as entropy and can be transported with flow inwardly rather than immediately being radiated away from the system. Consequently, the flow temperature becomes extremely high and nearly reaches the virial temperature. As a result, the disk can radiate high-energy emission such as gamma-rays (see Kato et al. 2008; Yuan & Narayan 2014 for more details). The disks and flows with this essential feature are called optically thin advection-dominated accretion flows (ADAFs). Historically, the significance of advection energy in hot accretion flows was first recognized by Ichimaru (1977) and more importantly, a wide range of studies on optically thin ADAFs has been performed by Narayan & Yi (1994, 1995a, 1995b) and Abramowicz et al. (1995) where the disk was thermally stable (more details in Yuan & Narayan 2014).

It should also be mentioned that in the field of hot accretion flows, many numerical hydrodynamic (HD) and MHD simulations have been carried out to investigate the dynamics of hot accretion flows and one of the most important findings by those simulations is that the mass inflow rate decreases inwardly (e.g., Igumenshchev & Abramowicz 1999, 2000; Stone et al. 1999; Hawley et al. 2001; De Villiers et al. 2003; Igumenshchev et al. 2003; Yuan & Bu 2010; Pang et al. 2011; Yuan et al. 2012a, 2012b; Bu et al. 2013), and it is not constant as was previously believed. Following those simulation results, one- and two-dimensional self-similar solutions of ADAFs in the presence of outflow and a magnetic field have been performed (e.g., Xu & Chen 1997; Blandford & Begelman 1999, 2004; Xue & Wang 2005; Akizuki & Fukue 2006; Abbassi et al. 2008; Zhang & Dai 2008; Bu et al. 2009; Jiao & Wu 2011; Abbassi & Mosallanezhad 2012; Mosallanezhad et al. 2013, 2014; Samadi et al. 2015). Note that the properties and dynamics of the hot accretion flows with a magnetic field and outflow is beyond the scope of this work.

In the optically thin ADAFs, the accretion rate is very low, $\dot{M} \lesssim 0.1 L_{\rm Edd}/c^2$, where $L_{\rm Edd}$ is the Eddington luminosity and $c$ is the speed of light. In addition, the optically thin ADAFs are geometrically thick disks, i.e., $H/R \lesssim 1$, where $H$ is the disk's scale height and $R$ is the radius in cylindrical coordinates. It should be noted here that in the novel vertically averaged self-similar methodology presented by Narayan & Yi (1994, hereafter NY94), the energy equation expressed as

$$q^{\rm adv} = q^+ - q^- \equiv f q^+, \tag{1}$$

where $q^{\rm adv}$ represents the rate of the entropy advection in the radial direction, i.e., $\rho v_{\rm r} T ds/dR$, $\rho$ is the density of the gas at the equatorial plane of the disk, $v_{\rm r}$ is the radial velocity, and s and T are the specific entropy and temperature of the gas, respectively. In Equation (1), $q^+$ gives the total heat generated by viscosity per unit volume per unit time in the radial direction. They defined the advection parameter as $f \equiv q^{\rm adv}/q^+$, which measures the fraction of the advection energy stored as entropy. Consequently, $(1 - f)$ will be radiated away from the system. They integrated the flow equation in the vertical direction. Making the usual assumptions such as steady state, axisymmety, and □-viscosity, they obtained a set of ordinary differential equations for the variables as a function of r. They have shown that the equation has an exact self-similar solution where all variables have power-law dependencies on r. Vertical integration is a standard approximation that has been used for thin disks where the vertical thickness is usually much smaller than the local radius. However, as we mentioned, optically thin ADAFs are

geometrically thick disks, therefore the height-integrated approximation is not appropriate because the physical variables are not only a function of r but they should also be a function of the vertical direction, □. Then, in the case of optically thin ADAFs, the 1D approach is not suitable. Later on, Narayan & Yi (1995a, hereafter NY95a) tried to solve the HD equations in spherical polar coordinates $(r, \theta)$ with radially self-similar solutions but their results only corresponded to the simplest form of the advection parameter, i.e., $f =$ constant.

To find how the advection parameter varies along the spherical polar angle, Gu et al. (2009) adopted a polytropic relation, $p = K\rho^{\Gamma}$, in the vertical direction which is normally used in the vertically integrated geometrically thick disk model (e.g., Kato et al. 2008). They defined the inclination $\theta_s$ near the polar axis as the surface of the disk. Therefore, the main conclusion was that the optically thin ADAFs are geometrically thick since the free surface of the disk is very close to the polar axis. By taking into account the effect of a toroidal magnetic field and its corresponding heating, Samadi et al. (2014) determined the thickness of ADAFs. Their results show that the vertical component of the magnetic force acts in the direction opposite to gravity and compresses the disk; thus, compared with the non-magnetic case, in general the disk half-thickness, $\Delta\theta$, is significantly reduced. It should be emphasized that in both the abovementioned works, the power index $\Gamma$ was considered to have a typical value above unity, for example, $\Gamma = 4/3$. Also, the constant $K$ is set equal to one, $K = 1.0$, to solve their one-boundary differential equations starting from the surface of the disk. Simulations carried out by De Villiers et al. (2005) revealed that the time-averaged density drops faster than the pressure in the vertical direction, which means that the power index $\Gamma$ should be less than one to satisfy the polytropic relation in the $\theta$ direction.

A few analytical solutions in the case of hot accretion have been presented and such solutions need to assume some simplifications. For instance, Shadmehri (2014) considerd the energy equation of the gas with the inclusion of only the $\tau_{r\phi}$ component of viscosity in the viscous energy dissipation term and found a very creative analytical solution. Later, based on the new simulation results mentioned above, Gu (2015, hereafter G15) repeated his previous work, Gu et al. (2009), with the new idea of finding an analytical solution. The behavior of physical variables is in satisfactory agreement with those in NY95a except for the variation of the isothermal sound speed and radial velocity profiles along the vertical direction. The main conclusion was that viscous heating and advection cooling cannot balance each other. Therefore, no thermal equilibrium exists under the purely inflow assumption.

The analytical solution we present here is from the same methodology as described in G15, with three modifications. First, we define the first boundary conditions at the rotation axis $\theta = 0°$ to increase the angular range of our calculation. We made this change because in terms of optically thin ADAFs, the disk is considered to be geometrically thick and there might exist low density with a high-temperature flow above the surface of the disk. Second, following NY95a, to avoid singularity at the poles, the disk is taken to be symmetric with respect to this axis. The second change leads to finding a relation between the value of constant $K$ and the density at the rotation axis. Finally, we will adopt the modified "$\alpha$" description of viscosity defined by Bisnovatyi-Kogan & Lovelace (2007). In the next section we explain with more details why this form of viscosity is needed. With the aforementioned modification, we can address whether there exists thermal equilibrium in the purely inflow case and check how the advection parameter changes along the vertical direction.

The outline of this paper is as follows. In Section 2, the basic equations and boundary conditions are introduced. The numerical results are shown and discussed in more detail in Section 3. Finally, a brief summary and conclusions will be given in Section 4.

## 2. BASIC EQUATIONS AND BOUNDARY CONDITIONS

### 2.1. Basic Equations

The standard HD equations are employed in the spherical coordinate system $(r, \theta, \phi)$ where the steady state accretion flow is taken to be axisymmetric (i.e., $\partial/\partial\phi = 0$). The gravitational potential of the central black hole is described in terms of the Newtonian potential, which is more convenient for the self-similar formalization, $\psi(r) = -(GM)/r$. In addition, the flow is in the non self-gravitating regime and initially the relativistic effects are neglected. Following NY95a, we assume $v_\theta = 0$, which corresponds to a hydrostatic equilibrium in the vertical direction. However, this assumption is not appropriate when investigating the effects of outflow on the dynamics of the accretion flow (see, e.g., Jiao & Wu 2011; Mosallanezhad et al. 2014 for more details). Therefore, the continuity equation and the three components of the equation of motion are as follows,

$$\frac{1}{r^2}\frac{\partial}{\partial r}\left(r^2\rho v_{\rm r}\right) = 0, \tag{2}$$

$$v_{\rm r}\frac{\partial v_{\rm r}}{\partial r} - \frac{v_\phi^2}{r} = -\frac{GM}{r^2} - \frac{1}{\rho}\frac{\partial p}{\partial r}, \tag{3}$$

$$v_\phi^2 \cot\theta = \frac{1}{\rho}\frac{\partial p}{\partial \theta}, \tag{4}$$

$$v_{\rm r}\frac{\partial v_\phi}{\partial r} + \frac{v_{\rm r} v_\phi}{r} = \frac{1}{\rho r^3}\frac{\partial}{\partial r}\left(r^3\tau_{r\phi}\right), \tag{5}$$

where $v_{\rm r}$ and $v_\phi$ are radial and azimuthal components of velocity, $\rho$ is the mass density, $p$ stands for the gas pressure, and in Equation (5), $\tau_{r\phi}$ represents the $r\phi$ component of the anomalous stress tensor. It should be emphasized that in a real case, the magnetic stress driven by the magneto-rotational instability (MRI) transfers the angular momentum outside the disk (Balbus & Hawley 1991, 1998). Since in our HD case we do not consider the magnetic field, the anomalous shear stress tensor has been considered to mimic the magnetic stress (see the HD simulations performed by Yuan et al. 2012a for more details). This parameter can be written as

$$\tau_{r\phi} = \mu r\frac{\partial}{\partial r}\left(\frac{v_\phi}{r}\right), \tag{6}$$

where $\mu(\equiv\nu\rho)$ is the viscosity coefficient, which determines the magnitude of the stress, and $\nu$ is called the kinematic viscosity coefficient. There are a lot of uncertainties about how to prescribe such a viscosity parameter. Most researchers adopt the "$\alpha$" description for standard thin disks introduced by Shakura & Sunyaev (1973), which is proportional to the speed of sound as $\nu = \alpha h c_{\rm s}$. Here, $h$ is the disk's scale height and $\alpha$ is

a constant parameter less than unity. We know that if the viscosity coefficient scales with radius as $\nu \propto r^{1/2}$ then radial self-similarity will be possible.

It should be pointed out that some simulations have been carried out for different forms of viscosity coefficients in accretion disks which found that the azimuthal components dominate other components (e.g., Stone et al. 1996); therefore, in HD calculations, it would be more convenient to take into account the azimuthal components (see Stone et al. 1999; Yuan et al. 2012a, 2012b).

NY95a obtained their solutions for the ADAF model corresponding to the usual "$\alpha$" description of viscosity. They also checked whether the results are sensitive to the viscosity by adopting a different form, $\nu = \alpha r c_s$, and concluded that their solutions with the new form are similar to those with the "$\alpha$" description. This prescription may not be suitable in a real case, since there exists a low-density corona above the disk with a nearly virial temperature. In addition, in the case of a geometrically thick and hot disk (ADAF model), the hottest temperature should be achieved at the rotation axis, $\theta = 0, \pi$ (see Figure 1 of NY95a for more details). On the other hand, the viscosity is due to MRI turbulence and this quantity should vanish at the surface of the disk (Bisnovatyi-Kogan & Lovelace 2007; Lovelace et al. 2009). Then, if the kinematic viscosity coefficient is proportional to the isothermal sound speed, $\nu \propto c_s$, then this quantity cannot vanish at the surface of the disk as MRI turbulence predicts.

In order to avoid the disparateness in terms of the turbulent viscosity, following Lovelace et al. (2009), we adopt the modified "$\alpha$" description of viscosity as

$$\nu = \alpha \frac{c_s^2}{\Omega_k} g(\theta). \tag{7}$$

In the above equation, $\Omega_K (\equiv \sqrt{GM/r^3})$ is the Keplerian angular velocity of the disk and $g(\theta)$ is a dimensionless function equal to unity and zero in the body and surface of the disk, respectively (e.g., Lovelace et al. 2009). For simplicity, we consider $g(\theta) = \sin\theta$ to satisfy the aforementioned conditions.

We are interested in investigating whether or not the advection parameter, $f$, which is normally considered to unity, $f = 1$, in the case of ADAF, remains constant along the polar angle (e.g., NY95a; Xu & Chen 1997; Jiao & Wu 2011). Therefore, following Gu et al. (2009) and Gu15, we apply the polytropic relation, $p = K\rho^\Gamma$, in the $\theta$ direction as our last equation. Although they obtained solutions by fixing $K = 1$, we explain how this constant parameter will be determined in the next section. We also note that the simulations of De Villiers et al. (2005) revealed that the power index $\Gamma$ is less than unity. This is mainly important because their results show that the time-averaged density drops faster than pressure from the equatorial plane to the polar axis. Based on those results, $\Gamma$ is set to be less than one throughout this paper.

We adopt self-similar solutions in the radial direction to simplify the equations as

$$\rho(r, \theta) = \rho(\theta) r^{-3/2}, \tag{8}$$

$$v_r(r, \theta) = \sqrt{\frac{GM}{r}} v_r(\theta) = v_K(r) v_r(\theta), \tag{9}$$

$$v_\phi(r, \theta) = v_K(r) v_\phi(\theta), \tag{10}$$

$$p(r, \theta) = p(\theta) GM r^{-5/2}. \tag{11}$$

By substituting the above self-similar solutions into Equations (2)–(5), they will be reduced to

$$-\frac{1}{2} v_r(\theta)^2 - v_\phi(\theta)^2 = -1 + \frac{5}{2} K \rho(\theta)^{\Gamma-1}, \tag{12}$$

$$v_\phi(\theta)^2 \cot\theta = K\Gamma \rho(\theta)^{\Gamma-2} \frac{d\rho(\theta)}{d\theta}, \tag{13}$$

$$v_r(\theta) = -\frac{3}{2} \alpha K \rho(\theta)^{\Gamma-1} \sin\theta. \tag{14}$$

We will put Equations (12) and (14) into (13) in order to obtain the differential equation for the density. Before doing that, it should be noted that the first term on the left-hand side of Equation (12) is very small compared to the other terms. This is because, in the case of ADAF, the radial velocity is very low and the viscosity constant considered here is fixed as $\alpha = 0.1$ (see Equation (14)). Hence, without any significant change in our results we can neglect this term and, therefore, the differential equation will be written as (see G15 for more details)

$$\frac{d\rho(\theta)}{d\theta} = \frac{\cot\theta}{\Gamma} \left( \frac{\rho(\theta)^{2-\Gamma}}{K} - \frac{5}{2} \rho(\theta) \right). \tag{15}$$

The above differential equation has an analytical solution that will be obtained after introducing the boundary conditions in the following section.

### 2.2. Boundary Conditions

We define the boundary conditions at the rotation axis $\theta = 0$ and equatorial plane $\theta = \pi/2$ to occupy the angular range $0 \leqslant \theta \leqslant \pi/2$. Following NY95a, to avoid singularity at the polar axis, we assume the boundary condition to be

$$\theta = 0: \qquad \frac{d\rho}{d\theta} = 0. \tag{16}$$

The above boundary condition leads to a value of constant $K$. Therefore, in Equation (15), the term inside the parentheses should become zero to satisfy the above boundary condition. So, the $K$ parameter can be derived as

$$K = \left(\frac{2}{5}\right) \rho_0^{1-\Gamma} \tag{17}$$

where $\rho_0$ represents the value of the density at the rotation axis. Figure 1 shows the variation of constant $K$ versus $\Gamma$ corresponding to different values of $\rho_0$. Note that since we will fix the value of the density at the equatorial plane to unity, $\rho(\pi/2) = 1.0$, the magnitude of $\rho_0$ in our figures represents the ratio of the density at the polar axis to the midplane of the disk. It is clear from Equation (17) and also Figure 1 that $K$ increases with increasing power index $\Gamma$ for different fixed values of $\rho_0$. Another feature that can be seen in this figure is that the value of $K$ cannot exceed $2/5$, which is the higher limit of this parameter with the $\Gamma$ index in the range $0 < \Gamma < 1.0$. As we explained before, we consider this range for $\Gamma$ because according to the simulation results carried out by De Villiers et al. (2005) the time-averaged density drops faster than pressure in the $\theta$ direction. This figure is compared with Figure

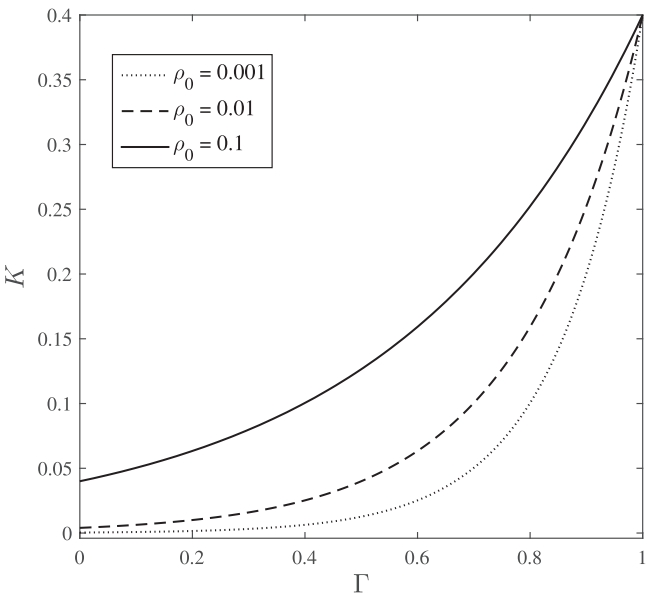


**Figure 1.** Variation of $K$ with $\Gamma$ for different values of density at the polar axis, $\rho = 0.001, 0.01, 0.1$.

2 in G15 because at first we decided to modify G15. Comparing Equation (17) with Equation (10) from G15, obviously both will be equal if one considers the surface angle to be 0°. In order to avoid defining the parameter $\lambda(\equiv(p_0/\rho_0)/v_K^2)$ as the energy advection on the midplane of the disk (G15), we instead use the constant $K$, which is the coefficient inside the polytropic equation.

Now we turn our attention to finding an analytical solution for the density in the vertical direction. By integrating Equation (15) along the $\theta$ direction, we can easily obtain the density profile as

$$\rho(\theta) = \left\{ \frac{1}{5K}\left[ \left(5K\rho(\pi/2)^{\Gamma-1} - 2\right) \sin\theta^{\frac{-5(\Gamma-1)}{2\Gamma}} + 2 \right] \right\}^{\frac{1}{\Gamma-1}} \tag{18}$$

where the value of the density at the equatorial plane is set to be $\rho(\pi/2) = 1.0$ throughout this paper. To complete the specification of the results, we need to define the advection parameter, $f^{\rm adv}$. In the self-similar formalism, the advective cooling rate and the viscous heating rate per unit volume can be expressed as

$$q^{\rm adv} = -\frac{5-3\gamma}{2(\gamma-1)}\frac{pv_{\rm r}}{r}, \tag{19}$$

$$q^{+} = \frac{9\alpha}{4}\frac{pv_\phi^2}{rv_K}\sin\theta. \tag{20}$$

Therefore, by vertical integration over $q^{\rm adv}$ and $q^+$, we can obtain $Q^{\rm adv}$ and also $Q^+$ as

$$Q^{\rm adv} = 2\int_0^{\frac{\pi}{2}} q^{\rm adv} r \sin\theta \, d\theta \tag{21}$$

$$Q^{+} = 2\int_0^{\frac{\pi}{2}} q^{+} r \sin\theta \, d\theta. \tag{22}$$

Then, the energy advection factor is given by $f^{\rm adv} \equiv Q^{\rm adv}/Q^+$. In the next section we will show the behavior of all variables and also the variation of advection cooling and viscous heating by explanation and comparing our results to those in Gu15 and Gu et al. (2009).

## 3. NUMERICAL RESULTS AND DISCUSSION

In this section, we first study the angular distribution of the dynamical quantities derived from Equations (12)–(14) and (18). Figure 2 shows the variation of physical quantities with the polar angle using $\Gamma = 0.75, 0.85, 0.95$ as three typical examples and a density at the polar axis of $\rho_0 = 0.01$. The dimensionless radial velocity, $v_{\rm r}/v_K$, is plotted in the top left panel of Figure 2. As can be seen, the radial velocity increases from the rotation axis to the equatorial plane. Actually, $v_{\rm r}$ is zero at $\theta = 0°$ and reaches its maximum at $\theta = \pi/2$ for all $\Gamma$ power index values. It should be noted here that, in terms of $\Gamma < 1$, G15 found that the radial velocity increases toward the rotation axis (see Figure 1, panel (b) of G15). This contradiction is simply because in this paper the modified form of the $\alpha$ prescription for viscosity is adopted (see Equation (7) and also Equation (14) for more details). In addition, our result shows that the larger $\Gamma$ leads $v_{\rm r}$ to increase further.

The top right panel displays the dimensionless azimuthal velocity, i.e., $v_\phi/v_K$. It is clear that $v_\phi$ increases from $\theta = 0°$ to $\theta = \pi/2$ and very close to the pole, $v_\phi$ vanishes and becomes zero. This behavior is clearly because, as a second modification to G15, the disk is taken to be symmetric with respect to the polar axis. As a result, the centrifugal force will become zero at the rotation axis. Moreover, the azimuthal component of the velocity is larger for small values of $\Gamma$. In fact, the largest variation of $v_\phi$ belongs to the smaller value of $\Gamma$. As seen in this panel $v_\phi$ is changed from $v_\phi = 0$ to just above $v_\phi = 0.8$ for $\Gamma = 0.75$.

The bottom left panel shows the vertical profile of the density $\rho$. It should be emphasized that the density profile is scaled with the density value on the equatorial plane of the disk. In this figure, the minimum value of the density at the rotation axis is considered to be $\rho_0 = 0.01$. As an overall trend, it is clear that the density increases from $\rho \simeq 0$ at the rotation axis to $\rho = 1$ at the equatorial plane. What is more, for larger $\Gamma$, $\rho$ increases sharper than for smaller ones, which means there exists extremely dense flow near the rotation axis, and the disk is considered to be geometrically thick.

Finally, the bottom right panel of Figure 2 shows the vertical variation of the isothermal sound speed, $c_{\rm s}^2$. As illustrated in this panel, $c_{\rm s}^2$ has a decreasing trend from the rotation axis to the equatorial plane. Furthermore, from the figure it is clear that for the case with $\Gamma = 0.95$, $c_{\rm s}^2$ is almost independent of $\theta$. Also, the maximum variation of $c_{\rm s}^2$ belongs to $\Gamma = 0.75$, from $c_{\rm s}^2 \simeq 0.4$ at $\theta = 0$ (at nearly virial temperature) to about $c_{\rm s}^2 = 0.12$ at $\theta = \pi/2$. In this case, a small value of $\Gamma$ might correspond to the thin disk model with a hot corona above the disk. Most importantly, our results are totally in agreement with those presented in NY95a. In fact, we should mention that by using an analytical solution for the case of no-wind self-similar solutions, solving a system of complex ordinary deferential HD equations with two boundary conditions is not necessary (readers are referred to NY95a for more details).

As we explained before, the main purpose of this work is to check whether or not the advection parameter remains constant along the vertical direction. Figure 3 represents the variation of the energy advection factor, $f^{\rm adv}$ $(\equiv Q^{\rm adv}/Q^+)$, with $\Gamma$ in the

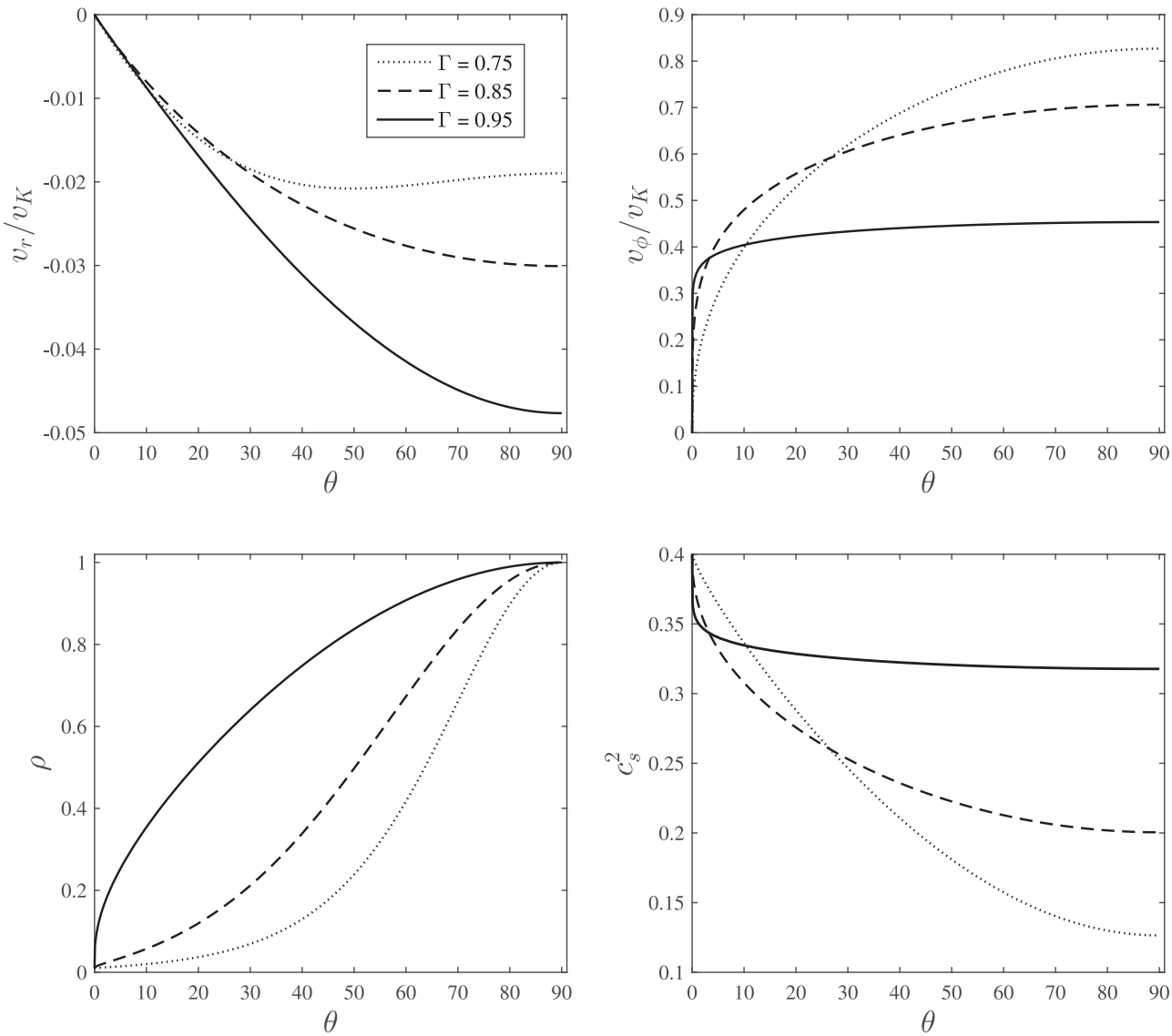


**Figure 2.** Variation of dimensionless physical quantities with polar angle $\theta$. The dotted, dashed, and solid lines correspond to $\Gamma = 0.75$, 0.85, 0.95, respectively. Here $\alpha = 0.1$ and $\rho_0 = 0.01$.

range $0.5 \leqslant \Gamma < 1$. In this figure the values of the density vary over the range, i.e., $\rho_0 = 0.001$, 0.01, 0.1. It is shown that $f^{\rm adv}$ increases with increasing $\Gamma$ and reaches unity for high values of $\Gamma$ corresponding to the fully advected case. In contrary to G15's conclusions, this figure obviously demonstrates that in the case of no outflow, i.e., $v_\theta = 0$, there exists thermal equilibrium and therefore, advection cooling can balance viscous heating. Also, it can be seen that for three typical density values on the rotation axis, full advection takes place when $\Gamma \simeq 0.95$. Therefore, Figure 1, together with this figure, shows that when the energy equation is replaced with the polytropic equation of state, $p = K\rho^\Gamma$, the fully advected case will be possible if constants $K$ and $\Gamma$ vary only in the range $0 < K \leqslant 0.4$ and $0.5 \leqslant \Gamma < 1$, respectively.

Finally, the vertical variation of the advection factor, $f(\theta) = q^{\rm adv}/q^{\rm vis}$ (the ratio of advection cooling to the viscous heating per unit volume), is plotted in Figure 4 for the same three values of the density in Figure 3 with $\Gamma = 0.95$. It can be seen that the value of the energy advection factor is not constant in the $\theta$ direction and increases from the equatorial plane toward the rotation axis. In addition, a lower value of the polar axis density causes a smaller value of $f(\theta)$. It is also seen that the energy advection factor is below unity, i.e., $f(\theta) \lesssim 1$ for $\rho = 0.001$. What is more, for the case with $\rho = 0.01$ the value of the energy advection factor is first below unity and then becomes greater than one near the rotation axis. Furthermore, a larger value of the density close to the rotation axis, i.e., $\rho = 0.1$, causes an upper limit of $f(\theta)$, i.e., $f(\theta) \simeq 2.8$ at $\theta = 0$, and more importantly this factor is always above unity for the entire vertical range. Therefore, unlike NY95a's assumption, which was to adopt $f = 1.0$ throughout the angular direction, our result clearly indicates that the advection parameter is a function of $\theta$, i.e., $f(\theta)$, and may exceed unity in some cases.

## 4. SUMMARY AND CONCLUSIONS

In this paper, we tried to solve the HD equations of optically thin ADAFs in the spherical coordinate system ($r$, $\theta$, $\phi$), where the steady accretion disk is considered to be symmetric with respect to the rotation axis as well as the equatorial plane. The

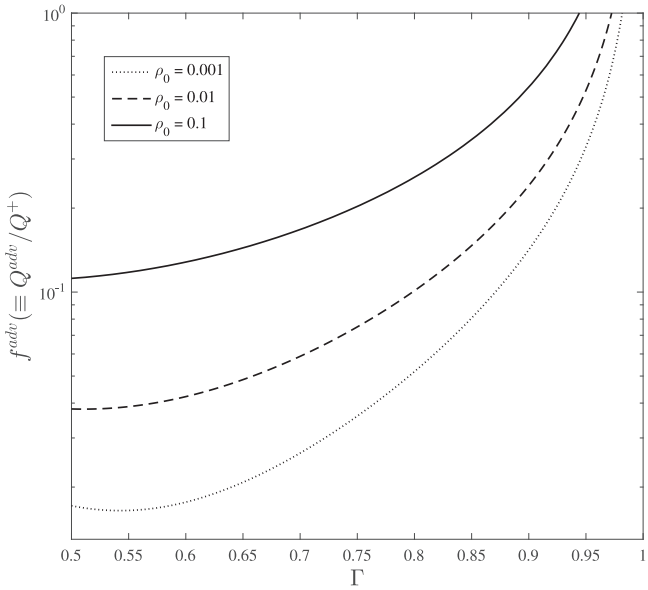


**Figure 3.** Variation of the energy advection factor, $f^{\rm adv}$ ($\equiv Q^{\rm adv}/Q^+$), with $\Gamma$. The dotted, dashed, and solid lines correspond to $\rho_0 = 0.001$, 0.01, 0.1, respectively, with $\alpha = 0.1$.

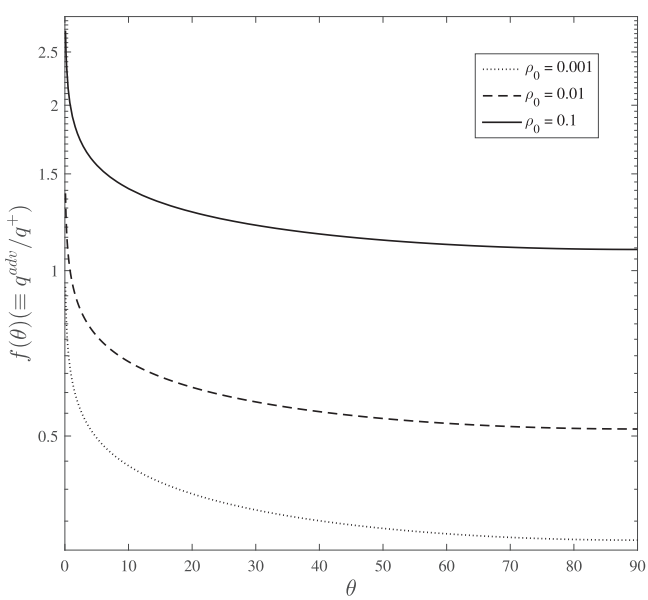


**Figure 4.** Vertical profile of the energy advection factor, $f(\theta)(\equiv q^{\rm adv}/q^+)$. The dotted, dashed, and solid lines correspond to $\rho_0 = 0.001$, 0.01, 0.1, respectively. Here, $\Gamma = 0.95$ and $\alpha = 0.1$.

central black hole gravity is described as the Newtonian potential, since this form is more convenient in the self-similar solutions, $\psi(r) = -(GM)/r$. In addition, instead of using the energy equation with a constant value for the advection parameter, $f$, following Gu et al. (2009) and G15, we adopted the polytropic relation in the vertical direction as $p = K\rho^\Gamma$. Compared with G15, we made three modifications. First, the vertical range of the calculation is enhanced from the rotation axis $\theta = 0°$ to the equatorial plane of the disk, $\theta = \pi/2$. This change has been made because in optically thin ADAFs the disk is geometrically thick, i.e., $H/R \lesssim 1$. Second, following NY95a, to avoid singularity at the pole, the disk is taken to be symmetric with respect to this rotation axis. This change causes us to find a relation between the value of constant $K$ and the density at the rotation pole. Finally, the modified "$\alpha$" description of viscosity is adopted (see, e.g., Lovelace et al. 2009 for more details).

With the abovementioned modifications and following the G15 methodology, we find an analytical solution for optically thin ADAFs. The presented results showed that unlike G15, the radial velocity decreases toward the rotation axis for all $\Gamma$ values. In addition, $v_\phi$ becomes zero at the rotation pole, which is due to the second modification. Furthermore, $c_s^2$, as in NY95a, has a decreasing trend from $\theta = 0$ (virial temperature) to $\theta = \pi/2$.

In contrast to G15, our solution represents the existence of thermal equilibrium in the vertical direction without outflow emanating. So, advecting cooling can balance viscous heating effectively. Moreover, If a polytropic relation is used rather than the energy equation in the vertical direction for full advection, $K$ and $\Gamma$ should only be in the range $0 < K \leqslant 0.4$ and $0.5 \leqslant \Gamma < 1$, respectively. At last, the value of the energy advection factor is not constant in the $\theta$ direction and increases from the equatorial plane toward the rotation axis.

In spite of the simplicity of our model in viscosity and the disk itself, we think that the presented semi-analytical results give us a better understanding of such a complicated system. It is good to note here that some modifications can be applied to ameliorate this study. Regarding the radial self-similar approximation, it cannot ensure that this solution is relevant to real accretion flows. In addition, the Newtonian potential was taken into account rather than the Paczyński & Wiita potential to avoid the general relativity effects in the innermost region of the accretion disk. Not only should the $r\phi$ component of the viscous stress tensor, $\tau_{r\phi}$, be employed, but also other components such as $\tau_{\theta\phi}$ should be taken into consideration. However, the advection factor $f^{\rm adv}$ in the energy equation was found to be function of the vertical direction, but this parameter must be a function of the radial and more significantly the mass accretion rate of the disk, i.e., $\dot{m}$. To resolve the aformentioned remarks, considering the $v_\theta$ and also the $\tau_{\theta\phi}$ component of the stress tensor may give more promising results in future works.

The authors thank Amin Mosallanezhad for useful suggestions and discussions. We also appreciate the referee for thoughtful and constructive comments in the early version of the paper. This work was supported by Ferdowsi University of Mashhad under grant 3/37875 (1394/04/03).

## REFERENCES

Abbassi, S., Ghanbari, J., & Najjar, S. 2008, MNRAS, 388, 663
Abbassi, S., & Mosallanezhad, A. 2012, RAA, 12, 1625
Abramowicz, M. A. 1995, ApJL, 438, L37
Akizuki, C., & Fukue, J. 2006, PASJ, 58, 469
Balbus, S., & Hawley, J. 1991, ApJ, 376, 214
Balbus, S., & Hawley, J. 1998, RvMP, 70, 1
Bisnovatyi-Kogan, G. S., & Lovelace, R. V. E. 2007, ApJ, 667, 167
Blair, W. P., Raymond, J. C., Dupree, A. K., et al. 1984, ApJ, 278, 270
Blandford, R. D., & Begelman, M. C. 1999, MNRAS, 303, L1
Blandford, R. D., & Begelman, M. C. 2004, MNRAS, 349, 68
Bu, D., Yuan, F., & Xie, F. 2009, MNRAS, 392, 325
Bu, D-F., Yuan, F., Wu, M., & Cuadra, J. 2013, MNRS, 434, 1692B
De Villiers, J. P., Hawley, J. F., & Krolik, J. H. 2003, ApJ, 599, 1238
De Villiers, J.-P., Hawley, J. F., Krolik, J. H., & Hirose, S. 2005, ApJ, 620, 878
Gu, W.-M. 2015, ApJ, 799, 71
Gu, W.-M., Xue, L., Liu, T., & Lu, J.-F. 2009, PASJ, 61, 1313
Hawley, J. F., Balbus, S. A., & Stone, J. M. 2001, ApJL, 554, L49
Ichimaru, S. 1977, ApJ, 214, 840

Igumenshchev, I. V., & Abramowicz, M. A. 1999, MNRAS, 303, 309
Igumenshchev, I. V., & Abramowicz, M. A. 2000, ApJS, 130, 463
Igumenshchev, I. V., Narayan, R., & Abramowicz, M. A. 2003, ApJ, 592, 1042
Jiao, C. L., & Wu, X. B. 2011, ApJ, 733, 112
Jimenez-Garate, M. A., Raymond, J. C., Liedahl, D. A., & Hailey, C. J. 2005, ApJ, 625, 931
Kato, S., Fukue, J., & Mineshige, S. 2008, Black-Hole Accretion Disks: Towards a New Paradigm (Kyoto: Kyoto Univ. Press)
Lovelace, R. V. E., Bisnovatyi-Kogan, G. S., & Rothstein, D. M. 2009, NPGeo, 16, 77
Mosallanezhad, A., Abbassi, S., & Beiranvand, N. 2014, MNRAS, 437, 3112
Mosallanezhad, A., Khajavi, M., & Abbassi, S. 2013, RAA, 13, 87M
Narayan, R., & Yi, I. 1994, ApJL, 428, L13 (NY94)
Narayan, R., & Yi, I. 1995a, ApJ, 444, 238 (NY95a)
Narayan, R., & Yi, I. 1995b, ApJ, 452, 710 (NY95b)
Pang, B., Pen, U.-L., Matzner, C. D., Green, S. R., & Liebendorfer, M. 2011, MNRAS, 415, 1228
Raymond, J. C. 1993, ApJ, 412, 267
Samadi, M., Abbassi, S., & Khajavi, M. 2014, MNRAS, 437, 3124
Shadmehri, M. 2014, MNRAS, 442, 3528
Shakura, N. I., & Sunyaev, R. A. 1973, A&A, 24, 337
Stone, J. M., Hawley, J. F., Gammie, C. F., & Balbus, S. A. 1996, Apj, 463, 656
Stone, J. M., Pringle, J. E., & Begelman, M. C. 1999, MNRAS, 310, 1002
Xu, G., & Chen, X. 1997, ApJL, 489, L29
Xue, L., & Wang, J.-C. 2005, ApJ, 623, 372
Yuan, F., & Bu, D. 2010, MNRAS, 408, 1051
Yuan, F., Bu, D., & Wu, M. 2012a, ApJ, 761, 130
Yuan, F., & Narayan, R. 2014, ARA&A, 52, 529
Yuan, F., Wu, M., & Bu, D. 2012b, ApJ, 761, 129
Zhang, D., & Dai, Z. G. 2008, MNRAS, 388, 1409